A Piezoresistive Micro Pressure Sensor Fabricated by Commercial DPDM CMOS Process

Lung-Jieh Yang[1]*, Chen-Chun Lai[3], Ching-Liang Dai[2], Pei-Zen Chang[3]

[1]*Department of Mechanical & Electro-Mechanical Engineering, Tamkang University Tamsui, Taiwan 251, R.O.C.*
[2]*Department of Mechanical Engineering, National Chung-Hsing University, Taichung, Taiwan 402, R.O.C.*
[3]*Institute of Applied Mechanics, National Taiwan University, Taipei, Taiwan 106, R.O.C.*

Abstract

A piezoresistive pressure sensor with a chip area of 2 mm × 4 mm has been fabricated by a standard CMOS process with additional MEMS post- process. The structure layers follow the design rules of the CMOS 0.8 μm DPDM (Double-Polysilicon-Double-Metal) multiple-project-wafer foundry service provided by the Chip Implementation Center, Taiwan. We used a finite element method software ANSYS to analyze the mechanical behavior of the pressure sensor and used the commercial software CADENCE to design the structure layout. After the CMOS process and the MEMS post- process, two CMOS pressure sensors with different diaphragm thickness were packaged and tested. The sensitivities of sensors were measured as 0.53 mV/atm/V and 13.1 mV/atm/V with non-linearity less than 5% (FSO), and agree with the theoretical prediction qualitatively.

***Key Words*:** CMOS, MEMS, Post Process, Pressure Sensor

1. Introduction

For the great progress of MEMS (Micro-Electro-Mechanical Systems) [1] in recent years, there are at least four kinds of processing methods including silicon bulk micro-machining, silicon surface micro-machining, LIGA [2] and CMOS (complementary metal-oxide-semiconductor) process [3] to fabricate the micro-sensors at present. Among these technologies, CMOS process for micro-sensors has the advantages of the maturity in IC (integrated circuit) foundry, the sub-micrometer spatial resolution of device fabrication and the functionality of on-chip circuitry.

CMOS layers were successfully used as the mechanical structures or the sensing elements of accelerometers, thermal sensors, magnetic sensors and pressure sensors [3–4]. Huang et al. [5] also designed a magnetic Hall sensor by the standard SPDM (single-polysilicon-double-metal) CMOS foundry service provided by the Chip Implementation Center (CIC), Taiwan, without post-processing. However, it caused some difficulties in achieving the design and the fabrication of the CMOS mechanical sensors due to the violations of some electric rules provided by the CMOS foundry line and the uncertainty of post-processing used to form the special geometry of sensor chip.

In this paper, we describe how to fabricate a CMOS piezoresistive pressure sensor under CIC's approval of altering some CMOS circuit checking sequences. Additionally, the designs of pressure sensors, the MEMS post-process of silicon anisotropic wet etching and the testing results with theoretical verification are also discussed.

2. Design of CMOS Piezoresistive Pressure Sensors

A pressure sensor is basically composed of a dia-

*Corresponding author. E-mail: ljyang@mail.tku.edu.tw

phragm structure and certain sensing elements corresponding to their sensing principles, e.g., capacitive effect, piezoelectric effect or piezoresistive effect. In this paper, we chose piezoresistive effect as the sensing principle of semiconductor pressure sensors for its simplicity both in fabrication and measurement.

When a pressure difference is applied on a pressure sensor, the diaphragm of the sensor will deform and induce bending stresses. It was shown that there is a contribution to resistance change from plane stresses that are longitudinal (σ_l) and transverse (σ_t) with respect to the orientation of current flow in piezoresistors. If the piezoresistor is so small as to have constant mechanical stresses inside itself, the total resistance change ΔR is given as follows [6].

$$\frac{\Delta R}{R} = (\pi_t \sigma_t + \pi_l \sigma_l) \tag{1}$$

where R is the original resistance of the piezoresistors subject to no pressure loading. Coefficients π_t and π_l are the transverse and the longitudinal piezoresistive coefficients which depend on the crystal orientation and the dopant types of piezoresistors. However, if the piezoresistive material is not mono-crystalline, e.g., doped polysilicon in this paper, the π coefficients should be modified to a simpler form [7].

We used the Wheatstone bridge configuration of piezoresistors to convert the resistance change directly into an output voltage signal. If we assume that the four piezoresistors in the Wheatstone bridge subject to a bias voltage V_b are ideally balanced and all have a resistance change ΔR, then a differential voltage output ΔV will be easily obtained by the following equation [6].

$$\frac{\Delta V}{V_b} = \frac{\Delta R}{R} \tag{2}$$

For a thin diaphragm of square-shape obeying the linear assumption of small deformation, the bending stresses σ_x and σ_y can be deduced from the vertical deflection which is a linear function of the applied pressure load P [8]. By the dimensionless analysis depicted in the appendix, we got a linear relation between P and σ_x, σ_y.

$$\sigma_x = \alpha\left(\frac{x}{L}, \frac{y}{L}; \nu, E\right) \cdot \left(\frac{L}{h}\right)^2 \cdot P \tag{3}$$

$$\sigma_y = \beta\left(\frac{x}{L}, \frac{y}{L}; \nu, E\right) \cdot \left(\frac{L}{h}\right)^2 \cdot P \tag{4}$$

where the coefficients α and β vary only with mechanical properties Poisson ratio ν and Young modulus E, after the position of piezoresistors are assigned definitely. From (1) to (4), we can define the sensitivity S of the pressure sensor as the voltage changing rate per unit pressure therefore.

$$S = \frac{\left(\frac{\Delta V}{V_b}\right)}{P} = \left(\frac{L}{h}\right)^2 (\alpha\pi_t + \beta\pi_l) \tag{5}$$

From (5), we see that the sensitivity S is expressed as a function of diaphragm geometry and material properties in a separation form. The effect of diaphragm geometry can be extracted by the ratio of diaphragm width L and thickness h. On the other hand, the Young modulus E and Poisson ratio ν appeared in α and β are sufficient to define the material properties of the isotropic elastic material. Such an expression can quickly help us figure out how the sensitivity varies with different sensor designs. For example, if the materials for diaphragm structure and piezoresistors are given, equation (5) is regarded as a quadratic relation of parameter (L/h) only. It then reveals that a thinner or a wider diaphragm design is suitable for pressure sensors of high sensitivity with the beneficial merits of two orders of magnitude.

The CMOS layers provided by the standard 0.8 μm DPDM foundry service consist of two polysilicon layers, two metal (aluminum) layers, one passivation (PECVD silicon nitride) layer and other oxide layers. We used the passivation layer the oxide layer and one metal layer as the 4μm thick composite diaphragm with an area of 400 μm × 400 μm. The polysilicon material is arranged between two oxide layers and is used as the piezoresistors herein. The cross section of the pressure sensor is shown in Figure 1, while Figure 2 is the layout of the pressure sensor. To make sure that the diaphragm structure has be done exactly, all these layouts had been checked by the 0.8 μm design rules and were finally generated by the IC design software CADENCE.

In order to get the maximum signal from the pressure sensor, the polysilicon piezoresistors are noted to be located on the edge and to be arranged near the surface of

the diaphragm (where the lower surface is chosen in this CMOS sensor design.) Such a recommendation is clarified by the basics of plate theory [8] or can be demonstrated by the finite element static analysis of the whole pressure sensor. Figure 3 is the numerical estimation of the distribution of the resistance changing rate all over the pressure diaphragm simulated by ANSYS.

We summarized the design procedures of a CMOS pressure sensor in Figure 4. This procedure made a success by CIC's approval of simplifying the verification sequence of a CMOS sensor to design rule check (DRC) only. There is no need for the sensor device to go through the electric rule check (ERC) or even the schematic design so far. The SEM pictures of the piezoresistive pressure sensor chip after CMOS foundry service is shown in Figure 5.

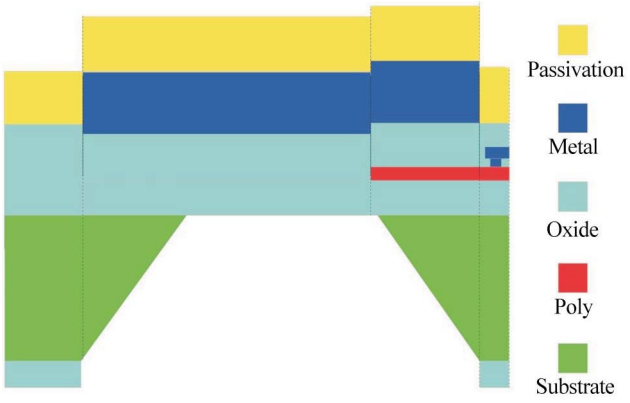

Figure 1. Cross section of the CMOS pressure sensor.

3. Design of MEMS Post-process

CMOS planar process makes composite layered structures of sensors only. It needs a MEMS post-process for completing the three-dimensional structure of the sensors. Sacrificial-layer removing or silicon etching on the front-side of silicon substrate is usually selected to release the levitation structures of accelerometers and thermal (infrared) sensors [3–4]. But for the requirement of air-sealing of the diaphragm structure herein, the anisotropic wet etching from the backside of the silicon substrate is chosen in this pressure sensor design. The followings depict the MEMS post-process.

First, we lapped and polished the backside of the substrate to reduce its thickness from 680 μm to 200 μm. This procedure decreases much time for chemical wet etching and preserves the aluminum pads which were exposed to the anisotropic etching solution from attacking

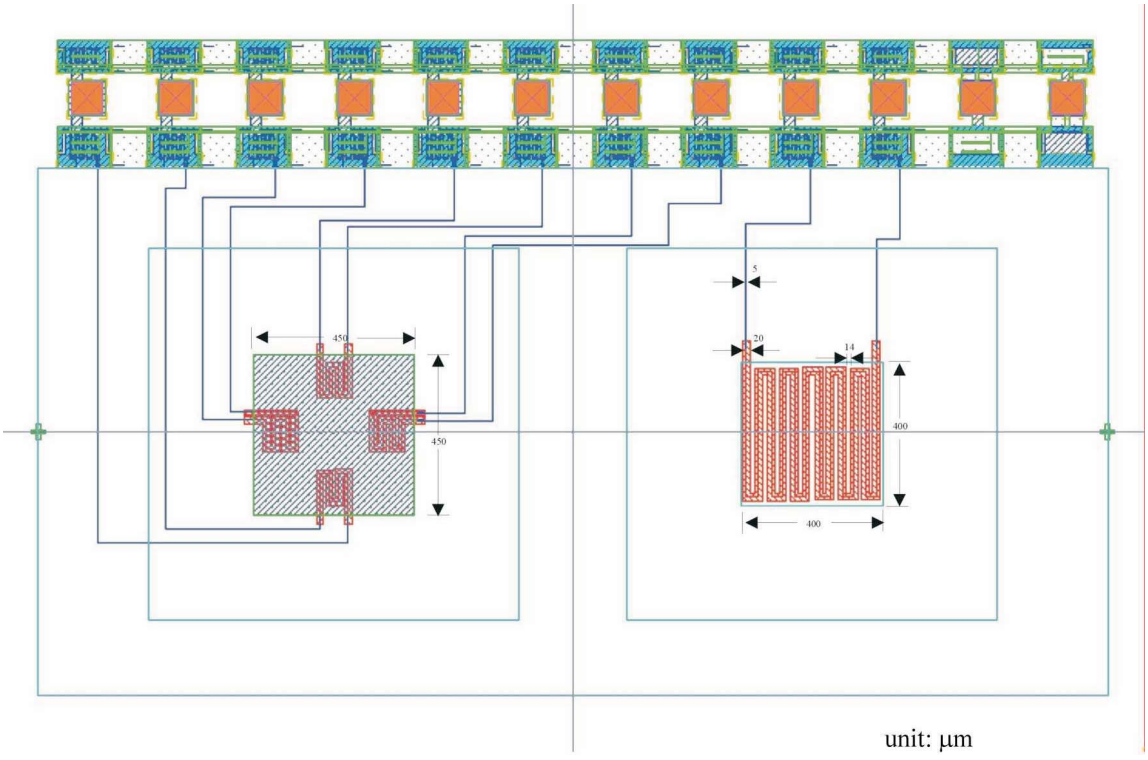

Figure 2. Layout of the CMOS pressure sensor.

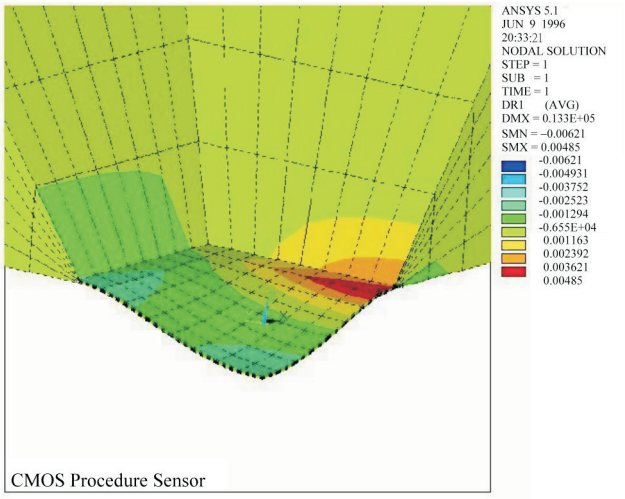

Figure 3. Distribution of the resistance changing rate of the CMOS pressure sensor (one quarter view).

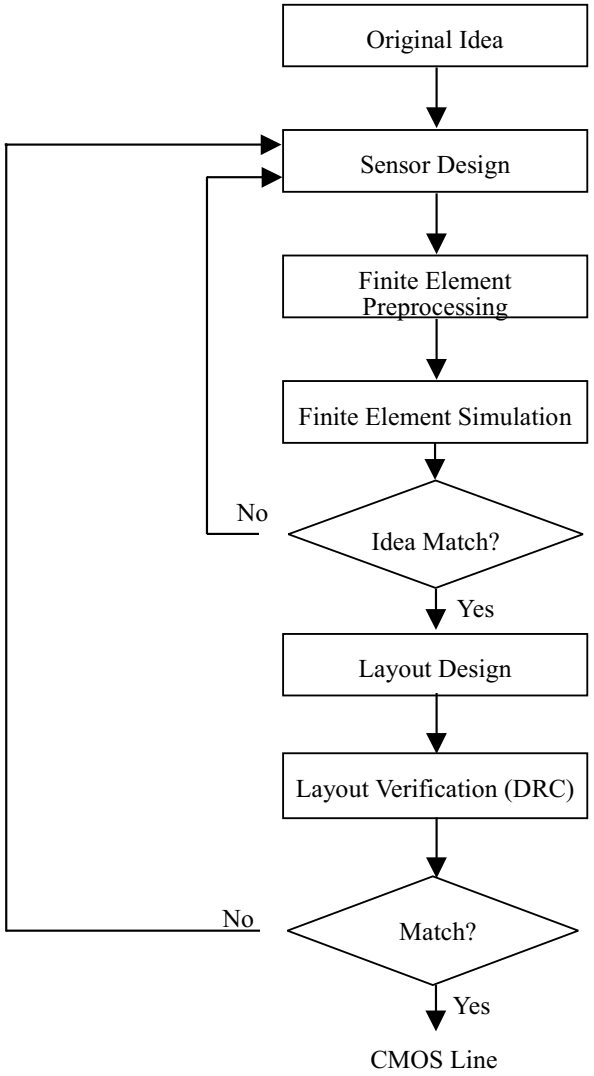

Figure 4. The flow chart for designing a CMOS pressure sensor.

too seriously.

Second, we chose low temperature thin film technology to deposit the etching masks on the backside of the substrate. These masks were 250°C PECVD silicon nitride film and sputtered silicon oxide film at room temperature. The thickness of PECVD silicon nitride is 0.4 mm and the sputtered silicon oxide is 1.2 mm thick. After the infrared double-sided lithography for photoresist preparation, the etching masking was patterned by RIE (reactive ion etching) with CF_4 plasma. The reason for the requirement of low temperature in MEMS post-process is that the aluminum layers of the CMOS process

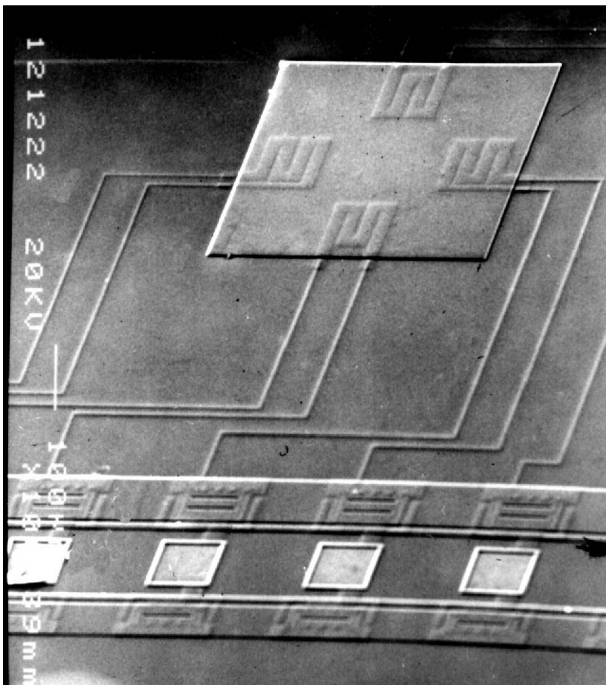

Figure 5. SEM photograph of the CMOS piezoresistive pressure sensor chip.

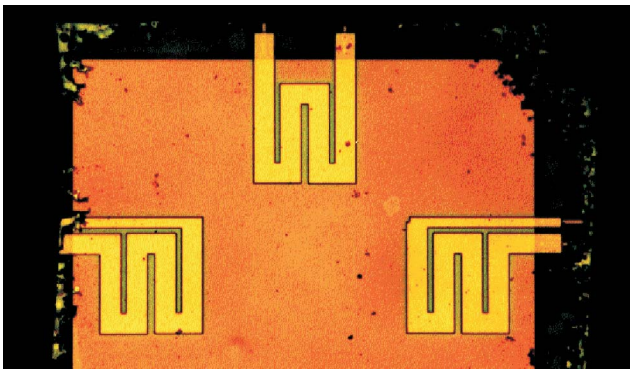

Figure 6. The backside picture of the sensor chip after MEMS post-process.

may have problems of spiking or short circuits in an environment with a temperature higher than 350°C.

Third, we selected EDP (ethylene-diamine: pyrocatechol: water = 1000 mL: 160 g: 320 mL) as the silicon anisotropic etching solution. Such a solution has good anisotropic character in etching the (100) silicon wafers, and it has good selectivity in metal preservation [6]. In our experiment, the EDP solution etches (100) silicon at 115 °C with an etch rate 1.25 μm/min [9] and the etch rate of EDP for aluminum is about 300 times lower than that of (100) silicon. Hence, the 0.6 μm thick metal pad was successfully preserved after the EDP etching. Figure 6 is the backside picture of the sensor chip with a 4 μm thick diaphragm after its post process.

4. Pressure Testing and Results

Two CMOS pressure sensors with different diaphragm thickness, 4 μm and 20 μm, were fabricated. The 20 μm thick diaphragm is composed of the 4μm thick CMOS structure and 16 μm thick silicon under the CMOS structure. Here, we assume the identical mechanical properties for silicon and CMOS layers, and there is five-folded variation in diaphragm thickness for the two fabricated CMOS pressure sensors.

After the wire bonding and the senor packaging, we fixed the bias voltage of Wheatstone bridge and let the testing pressure varied from 0 to an ultimate pressure corresponding to the diaphragm thickness. Figures 7 and 8 are the results of voltage outputs versus pressure loading for the two fabricated CMOS pressure sensors. The sensitivities are fitted as 0.530 mV/atm/V for 20 μm, and 13.1 mV/atm/V for 4 μm thick diaphragms with non-linearity less than 5% (FSO), respectively. Such data match the qualitative trend predicted by equation (5), i.e., a piezoresistive pressure sensor with one-fifth thickness of diaphragm has an output sensitivity of 25 times larger.

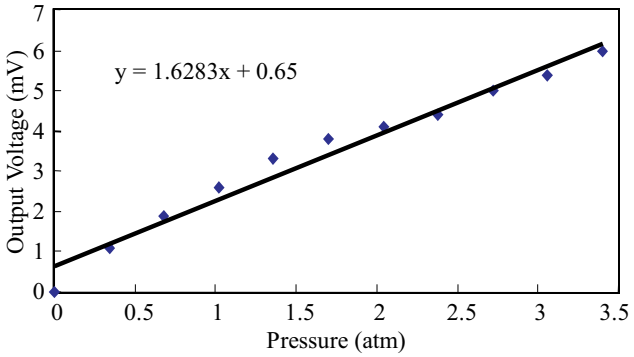

Figure 7. The output voltage vs. pressure for the sensor with 20 μm thick diaphragm; the bias voltage for the Wheatstone bridge is V_b = 3.07 V.

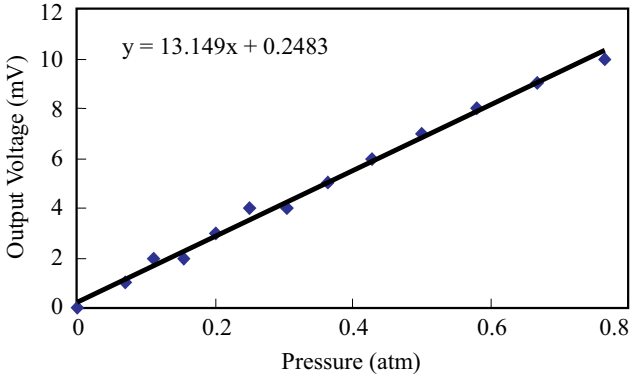

Figure 8. The output voltage vs. pressure for the sensor with 4 μm thick diaphragm; the bias voltage for the Wheatstone bridge is V_b=1.0 V.

5. Conclusions

We successfully fabricated CMOS piezoresistive pressure sensors by the commercial CMOS 0.8 μm DPDM process combined with MEMS post-process etching step. The sensitivity of a sensor with a 20 μm thick diaphragm is 0.530 mV/atm/V with pressure range from 0 to 3.4 atm, whereas the sensitivity of another sensor with a 4 μm thick diaphragm is 13.1 mV/atm/V with pressure range from 0 to 0.75 atm. These results agree with each other qualitatively by the theoretical prediction derived from the dimensionless analysis in this paper.

Acknowledgment

The authors wish to appreciate the Chip Implementation Center for supporting this project and offering much information and valuable recommendations. The helps from the Semiconductor Center in National Chiao-Tung University for providing the infrared double-side aligner, from the solid-state division of the Department of Electrical Engineering in National Taiwan University about the facility of post-process and from the Taiwan Silicon Microelectronics Corp. about the packaging service were all sincerely acknowledged.

Appendix

For a two-dimensional thin plate with the dimension of width L and thickness h, and with the material properties of isotropic, homogeneous characteristics, the vertical deflection function w(x, y; ν, E, L, h) satisfies the following governing equation with well-posed boundary conditions [10]:

$$D_x \frac{\partial^4 w}{\partial x^4} + 2H \frac{\partial^4 w}{\partial x^2 \partial y^2} + D_y \frac{\partial^4 w}{\partial y^4} = p \tag{A1}$$

$$\text{B.C.: } w = \frac{\partial w}{\partial n} = 0 \quad \text{on B} \tag{A2}$$

where $x \in (0,L)$, $y \in (0,L)$

where p denotes the external pressure loading, and the coefficients D_x, D_y and H denotes the rigidities of the elastic diaphragm with the function expression of E and ν shown as below.

$$D_x = D_y = D = \frac{Eh^3}{12(1-\nu^2)} \tag{A3}$$

$$H = D_1 = 2D_{xy} \tag{A4}$$

$$D_1 = \frac{\nu Eh^3}{12(1-\nu^2)} \tag{A5}$$

$$D_{xy} = \frac{Gh^3}{12(1-\nu^2)} \tag{A6}$$

The relations of plane stresses σ_x, σ_y with the deformation w(x, y) are listed as follows:

$$\sigma_x = -\frac{Ez}{1-\nu^2}\left(\frac{\partial^2 w}{\partial x^2} + \nu \frac{\partial^2 w}{\partial y^2}\right) \tag{A7}$$

$$\sigma_y = -\frac{Ez}{1-\nu^2}\left(\frac{\partial^2 w}{\partial y^2} + \nu \frac{\partial^2 w}{\partial x^2}\right) \tag{A8}$$

By the dimensionless analysis, we introduce following dimensionless variables to make equations (A1) (A-2) more neat for physical interpretation.

$$W = \frac{Dw}{pL^4} \tag{A9}$$

$$X = \frac{X}{L}, \; Y = \frac{y}{L} \tag{A10}$$

Inserting (A9) and (A10) into (A1) and (A2), we can obtain the dimensionless governing equation and its boundary conditions.

$$\frac{\partial^4 W}{\partial X^4} + 2\left(\frac{H}{D}\right)\frac{\partial^4 W}{\partial X^2 \partial Y^2} + \frac{\partial^4 W}{\partial Y^4} = 1 \tag{A11}$$

$$\text{B.C.: } W = \frac{\partial W}{\partial n} = 0 \quad \text{on B} \tag{A12}$$

where $X \in (0,1)$, $Y \in (0,1)$

We observe that equations (A11) and (A12) are all normalized with only one dimensionless parameter, the rigidity ratio (H/D), which correlates with material properties instead of the dimension of the thin plate. In other words, the vertical deflection W(X, Y) is determined by the material properties only, and has nothing to do with the dimension of the thin plate.

$$W(X, Y) = \hat{\alpha}(X, Y; H/D) \tag{A13}$$

Substitute (A9), (A10) and (A3) into (A13), the deflection functions W(X, Y) and w(x, y) become.

$$\begin{aligned} W(X,Y) &= \frac{D \cdot w(x,y;\nu,E,L,h)}{p \cdot L^4} \\ &= \frac{\left(\frac{Eh^3}{12(1-\nu^2)}\right) \cdot w(x,y;\nu,E,L,h)}{p \cdot L^4} \\ &= \hat{\alpha}\left(\frac{x}{L}, \frac{y}{L}; H/D\right) \\ &\Rightarrow w(x,y;\nu,E,L,h) = \hat{\alpha}\left(\frac{x}{L}, \frac{y}{L}; H/D\right)\frac{p}{E}\frac{L^4}{h^3} \end{aligned} \tag{A14}$$

Using (A7), (A8) and (A14), the equations (3) and (4) for maximum plane stresses (on the plate surface, z = h/2) σ_x, σ_y can be derived.

$$\begin{aligned} \sigma_x &= -6p\left(\frac{L}{h}\right)^2\left(\frac{\partial^2 W}{\partial X^2} + \nu \frac{\partial^2 W}{\partial Y^2}\right) \\ &= \alpha(X, Y; \nu, E) \cdot \left(\frac{L}{h}\right)^2 \cdot p \end{aligned}$$

$$\begin{aligned} \sigma_y &= -6p\left(\frac{L}{h}\right)^2\left(\frac{\partial^2 W}{\partial Y^2} + \nu \frac{\partial^2 W}{\partial X^2}\right) \\ &= \beta(X, Y; \nu, E) \cdot \left(\frac{L}{h}\right)^2 \cdot p \end{aligned}$$

References

[1] Leo, O'Connor, "MEMS-microelectromechanical System," *Mechanical Engineering*, Feb., pp. 40–47 (1992).

[2] Rogner, A., Eicher, J., Munchmeyer, D., Peters, R.-P. and Mohr, J., "The LIGA Technique-what Are the New Opportunities," *J. Micromech. Microeng*., Vol. 2, pp. 13−140 (1992).

[3] Baltes, H., "CMOS as Sensor Technology," *Sensors and Actuators*, A37-38, pp. 51−56 (1993).

[4] Warneke, B. and Pister, K. S. J., "In Situ Characterization of CMOS Post-process Micromachining," *Sensors and Actuator A: Physical,* Vol. 89, pp. 142−151 (2001).

[5] Yang, H. M. and Huang, Y. C., et al., "High Resolution MOS Magnetic Sensor with Thin Oxide in Submicron CMOS Process," *Sensors and Actuator A: Physical,* Vol. 57, pp. 9−13 (1996).

[6] Sze, S. M. (Ed.), *Semiconductor Sensor,* John Wiley & Sons, New York, U.S.A. (1994).

[7] Burns, D. W., et al., "Sealed-cavity Resonant Microbeam Pressure sensor," *Sensors and Actuator A: Physical,* Vol. 48, pp. 179−186 (1995).

[8] Timoshenko, S. and Woinowsky-Krieger, S., *Theory of Plates and Shell*, McGraw-Hill, New York, U.S.A. (1959).

[9] Petersen, K. E. "Silicon as a mechanical material," *Proc. IEEE*, Vol. 70, pp. 420−457 (1982).

[10] Bin, T. Y. and Huang, R. S., "CAPSS: a Thin Diaphragm Capacitive Pressure Sensor Simulator," *Sensors and Actuators*, Vol. 11, pp. 1−12 (1987).

Received Dec. 3, 2004
Accepted Jan. 17, 2005